



Heriot-Watt University
Research Gateway

The remarkable influence of N,O-ligands in the assembly of a bis-calix[4]arene-supported $[Mn^{IV}_2Mn^{III}_{10}Mn^{II}_8]$ cluster

Citation for published version:

Coletta, M, Sanz, S, McCormick, LJ, Teat, SJ, Brechin, EK & Dalgarro, S, 2017, 'The remarkable influence of N,O-ligands in the assembly of a bis-calix[4]arene-supported $[Mn^{IV}_2Mn^{III}_{10}Mn^{II}_8]$ cluster', *Dalton Transactions*, vol. 46, no. 48, pp. 16807-16811. <https://doi.org/10.1039/C7DT04233G>

Digital Object Identifier (DOI):

[10.1039/C7DT04233G](https://doi.org/10.1039/C7DT04233G)

Link:

[Link to publication record in Heriot-Watt Research Portal](#)

Document Version:

Peer reviewed version

Published In:

Dalton Transactions

General rights

Copyright for the publications made accessible via Heriot-Watt Research Portal is retained by the author(s) and / or other copyright owners and it is a condition of accessing these publications that users recognise and abide by the legal requirements associated with these rights.

Take down policy

Heriot-Watt University has made every reasonable effort to ensure that the content in Heriot-Watt Research Portal complies with UK legislation. If you believe that the public display of this file breaches copyright please contact open.access@hw.ac.uk providing details, and we will remove access to the work immediately and investigate your claim.

The remarkable influence of *N,O*-ligands in the assembly of a bis-calix[4]arene-supported $[\text{Mn}^{\text{IV}}_2\text{Mn}^{\text{III}}_{10}\text{Mn}^{\text{II}}_8]$ cluster

Received 00th January 20xx,
Accepted 00th January 20xx

Marco Coletta,^a Sergio Sanz,^b Laura J. McCormick,^c Simon J. Teat,^c Euan K. Brechin*^b and Scott J. Dalgarno*^a

DOI: 10.1039/x0xx00000x

www.rsc.org/

Calix[4]arenes are versatile ligands, capable of supporting the formation of a wide variety of polymetallic clusters comprising 3*d*, 4*f* or 3*d*-4*f* metal ions. Calixarene-based metal ion fragments act as both bridging and structure capping moieties in these systems, and this behaviour is systematically extended upon moving to bis-calix[4]arene, a relatively new ligand in which two calix[4]arenes are tethered at the methylene bridge position. *N,O*-ligands greatly influence cluster formation with bis-calix[4]arene, affording a remarkable mixed-valence $[\text{Mn}^{\text{IV}}_2\text{Mn}^{\text{III}}_{10}\text{Mn}^{\text{II}}_8]$ cluster that displays coordination chemistry typical of each ligand type, but also new structure capping behaviour for the latter.

The ability to control both the structure and composition of large, multi-component polymetallic clusters of paramagnetic metal ions is a challenging synthetic goal; this has concomitant effects on the resulting magnetic properties of the system. Ligand design has played a crucial role in this regard as it allows one to exert influence through the incorporation of well-known coordination modes.¹ Amongst the plethora of ligands available for the synthesis of such high-spin clusters, the utilisation of tripodal supports bearing disparate functionalities represents a logical choice. *N,O*-Chelates have been widely employed in the synthesis of polymetallic clusters, taking advantage of their common coordination modes. This includes the use of unsubstituted and *N*-substituted diethanolamines² to obtain, for example, a heptanuclear, six-membered mixed-valence $\text{Mn}^{\text{III/II}}$ wheel in which Mn^{II} and Mn^{III} cations alternate around a central Mn^{II} cation (**1**, Fig. 1A).^{2a} Close inspection of these cluster topologies suggests that many can be visualised as being constructed from distorted-cubanes or, alternatively, fused butterflies.

The latter represents a topology often encountered in our research in which we have used methylene-bridged calix[4]arenes as ligands / cluster supports. These molecules (e.g. *p*-^tBu-calix[4]arene and *p*-H-calix[4]arene, hereafter collectively termed $\text{H}_4\text{C}[4]\text{s}$) have emerged as versatile platforms for the synthesis of polymetallic clusters, capable of affording a wide variety of different structural topologies depending on the nature of the metal ions present; markedly different structures result from the incorporation of 3*d*,³ 4*f*,⁴ or 3*d* and 4*f* metal ions.⁵ From our work we have established a vast library of C[4]-supported metal clusters in which a recurring structural theme is that $[\text{C}[4]\text{TM}^{\text{III}}]$, $[\text{C}[4]\text{TM}^{\text{II}}]^{2-}$ or $[\text{C}[4]\text{Ln}^{\text{III}}]$ moieties act as bridges to metal ions within the cluster through their phenolate groups, but also as polyhedral capping fragments.⁶ With respect to the present contribution, particularly noteworthy systems resulting from these studies include a family of $[\text{Mn}^{\text{III}}_2\text{Mn}^{\text{II}}_2(\text{C}[4])_2]$ single molecule magnets^{3b,c} (SMMs, **2**, Fig. 1B) that feature the aforementioned butterfly-like cluster; in this case the oxidation state distribution is the reverse of those reported in the literature for other ligand types.⁷ A family of $[\text{Mn}^{\text{III}}_4\text{Ln}^{\text{III}}_4(\text{C}[4])_4]$ clusters was obtained in the presence of both TM and Ln ions, and these can be best described as four $[\text{Mn}^{\text{III}}(\text{C}[4])]$ moieties capping the edges of a Ln^{III} square ($\text{Ln} = \text{Gd}, \text{Tb}, \text{Dy}$).^{5a} Finally, $[\text{Ln}^{\text{III}}_6(\text{C}[4])_2]$ octahedra were isolated when the latter reaction was carried out in the absence of TM ions.⁴

It should be noted that the vast majority of the examples of C[4]-supported clusters outlined above were obtained under mild conditions,^{3b-d,4,5} but similar species can also be obtained using microwave^{3e,f} or solvothermal^{3a,8} synthesis. Markedly different structural topologies can be obtained when using Schlenk-line conditions, as this generally involves the use of bases that promote the incorporation of additional metal ions (e.g. alkali metals), dramatically affecting the resulting cluster topology.⁹ Thia-, sulfinyl-, and sulfonylcalix[4]arenes have also been used widely in cluster synthesis, and again, the prevailing coordination chemistry is drastically different to that found when using C[4]s as cluster supports; this is due to the

^a Institute of Chemical Sciences, Heriot-Watt University, Riccarton, Edinburgh, Scotland, EH14 4AS, UK. E-mail: S.J.Dalgarno@hw.ac.uk.

^b EastCHEM School of Chemistry, The University of Edinburgh, David Brewster Road, Edinburgh, Scotland, EH9 3FJ, UK. E-mail: ebrechin@ed.ac.uk.

^c Station 11.3.1, Advanced Light Source, Lawrence Berkeley National Laboratory, 1 Cyclotron Road, Berkeley, CA94720, USA.

[†] Electronic Supplementary Information (ESI) available: Additional figures relevant to discussion, table of bond lengths and bond valence sum (BVS) calculations. CCDC 1573336. For ESI and crystallographic data in CIF or other electronic format see DOI: 10.1039/x0xx00000x

incorporation of additional donor atoms in the ligand framework, the result of which is formation of common structural fragments comprising the relevant calixarene and four *3d*, *4f* or *3d-4f* metal ions. A detailed discussion of this vast coordination chemistry is far beyond the scope of this introduction, and for the sake of brevity the reader is directed to recent reviews on the topic,¹⁰ as well as examples of sulfonyl-C[4]-supported manganese clusters.¹¹

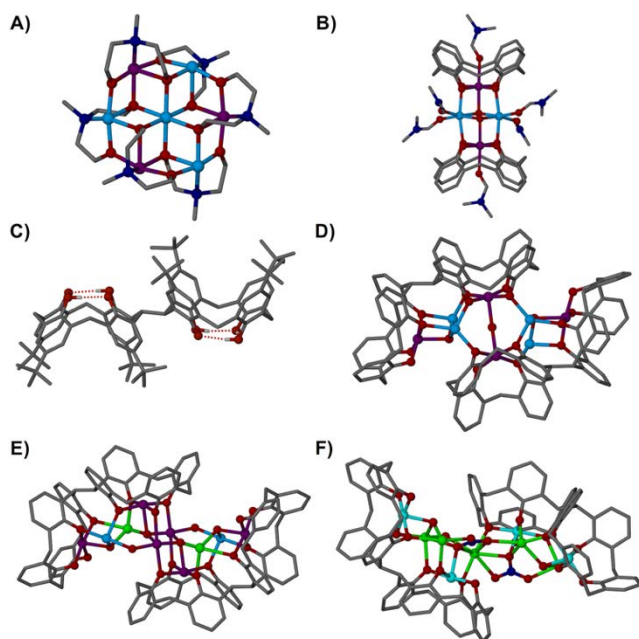


Fig. 1 Single crystal X-ray structures of **1** (A),^{2a} **2** (B),^{3b} H₈L1 (C),¹⁴ **3** (D),¹⁴ **4** (E),¹⁵ and **5** (F).¹⁶ Colour code C – grey, O – red, N – royal blue, Mn^{II} – pale blue, Mn^{III} – purple, Cu^{II} – light blue, Ln^{III} – green. Hydrogen atoms (except those involved in lower-rim H-bonding in C), ^tBu groups of C[4] and H₈L1 / L1 (except those shown in C), ligated solvent molecules in D, E and F, and co-crystallised solvent/anions omitted for clarity. Figures not to scale.

With the aforementioned coordination chemistry of C[4] in mind, we recently turned our attention to bis-*p*-^tBu-calix[4]arene (BisTBC[4], H₈L1, Fig. 1C), a relatively new ligand in which two H₄C[4]s are directly linked *via* a methylene bridge position.¹² Being conformationally mobile, we envisaged that it would act in a similar manner to H₄C[4], but that it would exhibit double structure capping behaviour and thus considerably enhance the nuclearity of any resulting polymetallic cluster.¹³ We recently reported the formation of a [Mn^{II}₄Mn^{IV}₄(L1)₂] cluster (**3**, Fig. 1D) in which the polymetallic core can be thought as two fused and highly distorted [Mn^{II}₂Mn^{IV}₂] butterflies.¹⁴ Perhaps the most important feature of this structure is the positions occupied by Mn^{II} ions, located in binding pockets between the constituent C[4] lower-rims that are generated by ligand inversion. A remarkably similar topology is encountered in a related [Mn^{II}₄Mn^{II}₂Ln^{III}₂(L1)₂] cluster, obtained *via* interchange of two Mn^{II} with Ln^{III} ions.¹⁴ Control over reactant stoichiometry afforded new clusters of formula [Mn^{II}₆Mn^{IV}₄(L1)₂] and [Mn^{II}₆Mn^{II}₂Ln^{III}₂(L1)₂] (**4**, Fig. 1E), and these were obtained *via* ‘insertion’ of two additional methoxy-bridged Mn^{III} ions to the [Mn^{II}₄Mn^{IV}₄(L1)₂] or

[Mn^{II}₄Mn^{II}₂Ln^{III}₂(L1)₂] cores.¹⁵ Our exploratory chemistry with H₈L1 also recently afforded a new family of clusters of general formula [TM^{III/II}_xLn^{III}_y(L1)_z] where the TM was Cu, Fe or Mn, the Ln was Gd, Tb or Dy, and the x:y ratio was 4:0, 5:4, 4:5 or 0:4 (e.g. **5**, Fig. 1F).¹⁶ Although these new clusters have rather different topologies, they all share common features that follow established binding rules and structural capping behaviours. In this contribution we report our initial findings from multi-component cluster-forming reactions incorporating an *N,O*-co-ligand as well as H₈L1 in a one-pot synthesis. The remarkable Mn₂₀ cluster formed displays coordination modes that are typical of both ligand types, but also features new structural behaviour for L1 which we attribute to the competitive metal ion binding nature of the co-ligand employed.

Reaction of 1:10:4 equivalents of H₈L1 with manganese(II) chloride tetrahydrate and diethanolamine (H₂DEA) in a DMF/MeOH mixture (to aid solubility) and in the presence of Et₃N (XS) as a base,¹⁷ afforded dark purple single crystals of [Mn^{IV}₂Mn^{III}₁₀Mn^{II}₈(L1)₂(DEA)₆(μ₄-O)₄(μ₃-O)₆(dmf)₁₀(Cl)₆(H₂O)₂](dmf)₂(MeOH)(H₂O)₃ (**6**, Fig. 2) upon vapour diffusion of Et₂O into the mother liquor.† The crystals were found to be in a monoclinic cell and structure solution was carried out in the space group *C2/c*. The asymmetric unit (ASU) comprises half of the reported formula, with ten Mn cations, two of which reside in the tetra-phenolato cavities in perfect accordance with the established binding rules for both C[4] and L1. The remaining eight cations propagate horizontally from L1, forming a polymetallic core supported by DEA molecules and bridging hydroxides / chlorides (Fig. 3A).

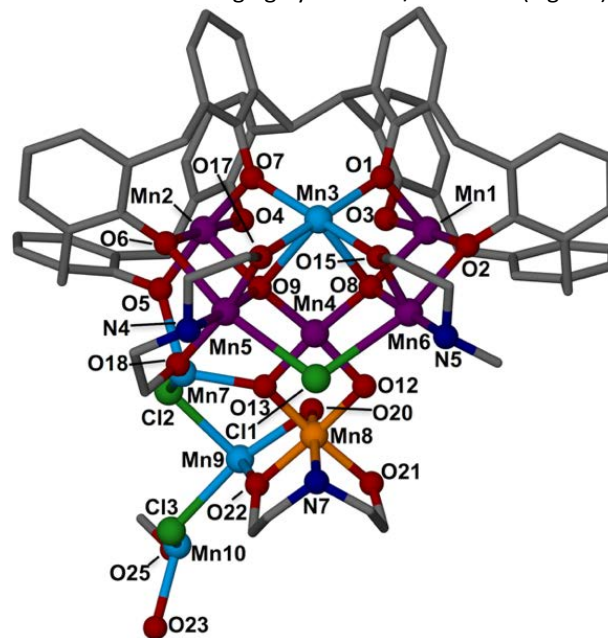


Fig. 2 Asymmetric unit in the single crystal X-ray structure of **6** with selected atoms labelled according to discussion. Colour code C – grey, O – red, N – royal blue, Mn^{II} – pale blue, Mn^{III} – purple, Mn^{IV} – orange, Cl – dark green. H atoms, ^tBu groups of L1, ligated solvent and co-crystallised solvent/anions are omitted.

Analysis of the structure shows a variety of coordination modes and oxidation states of the metal centres, the latter being confirmed by BVS calculations (Supporting Information).

Given the complexity of the structure it is necessary to include a detailed description of the coordination environment of the constituent metal ions. As expected, Mn1 is in the 3+ oxidation state and is bound in a C[4] lower-rim pocket described by O1–O4 (Mn–O distances in the range 1.892(4) – 1.967(3) Å). The coordination sphere of Mn1 is completed by a ligated dmf molecule residing in the C[4] cavity (Mn1–O10, 2.240(4) Å) and a μ_4 -oxide (Mn1–O8, 2.141(3) Å) which bridges to Mn3, Mn4 and Mn6 (Mn3–O8, 2.417(4) Å; Mn4–O8, 1.896(3) Å; Mn6–O8, 1.858(4) Å). The Jahn-Teller axis deviates from linearity and is defined by the O8–Mn1–O10 vector (170.79(15)°). Mn2, also in the 3+ oxidation state, has an analogous coordination environment, being bound to the lower-rim phenolic oxygens of one of the C[4] constituents of the L1 octa-anion (Mn2–O range 1.893(4) – 1.974(4) Å), a ligated dmf molecule (Mn2–O11, 2.250(3) Å) and a μ_4 -oxide (Mn2–O9, 2.117(3) Å), the latter of which bridges to Mn3, Mn4 and Mn5 (Mn3–O9, 2.504(4) Å; Mn4–O9, 1.888(3) Å; Mn5–O9, 1.848(4) Å). The Jahn-Teller axis shows similar deviation from linearity and is defined by the O11–Mn2–O9 vector (173.88(15)°). Mn3 is in the 2+ oxidation state, is hepta-coordinate, has distorted face-capped octahedral geometry and, in addition to the aforementioned μ_4 -oxide ligands, is also bound to two phenolic oxygens belonging to the C[4] moieties of L1 (Mn3–O1, 2.209(3) Å and Mn3–O7, 2.209(3) Å), a ligated dmf molecule (Mn3–O14, 2.200(3) Å) and two oxygens from different DEA ligands (Mn3–O15, 2.180(3) Å and Mn3–O17, 2.168(3) Å). Mn4 is in the 3+ oxidation state, is penta-coordinate and has a distorted square pyramidal geometry. The base of the pyramid is defined by the O8 and O9 μ_4 -oxides, as well as two μ_3 -oxides (Mn4–O12, 1.866(3) Å and Mn4–O13, 1.866(3) Å), whilst an oxo bridge is located at the apex (Mn4–O16, 2.284(3) Å). Mn5 is in the 3+ oxidation state, has distorted octahedral geometry and is bound to a μ -phenolate moiety (Mn5–O6, 2.232(3) Å), the O9 μ_4 -oxide, a chloride anion (Mn5–Cl1, 2.781(15) Å) that bridges to Mn6 (Mn6–Cl1, 2.827(15) Å) and a tridentate DEA ligand (Mn5–O17, 1.864(3) Å; Mn5–N4, 2.019(4) Å; Mn5–O18, 1.891(4) Å). The Jahn-Teller axis is located along the O6–Mn5–Cl1 vector and shows significant deviation from linearity (165.27(10)°). The coordination spheres of Mn2 (3+) and Mn6 (3+) are near identical to those of Mn1 (3+) and Mn5 (3+) respectively, with only negligible differences observed (Table S1); the Jahn-Teller axis for Mn6 is defined by the O2–Mn6–Cl1 vector (164.79(11)°), again showing deviation from linearity. Mn7 is in the 2+ oxidation state, is penta-coordinate and has distorted square pyramidal geometry. It is bound to a phenolic oxygen atom (Mn7–O5, 2.136(4) Å), a μ_3 -oxide (Mn7–O13, 2.028(3) Å), an oxygen of a ligated DEA (Mn7–O18, 2.135(4) Å), a ligated dmf molecule (Mn7–O19, 2.136(4) Å) and a μ -Cl (Mn7–Cl2, 2.521(14) Å) that bridges to Mn9. Mn8, Mn9 and their symmetry equivalent (s.e.) ions form a DEA-supported butterfly located at the centre of the large cluster, acting as a link between the two Mn₈ moieties (Fig. 3A). Mn8 is hexa-coordinate, is in a distorted octahedral geometry, and is in the 4+ oxidation state. Although not directly interacting with any calixarene moiety, this represents the first example in which a

Mn^{IV} is incorporated in an L1-supported cluster, along with frequently observed Mn^{III/II} ions. Mn8 is bound to three μ_3 -oxides (Mn8–O12, 1.820(3) Å; Mn8–O13, 1.828(3) Å; Mn8–O20, 1.917(3) Å) and a ligated DEA molecule (Mn8–O21, 1.925(4) Å; Mn8–N7, 2.041(4) Å; Mn8–O22, 1.923(3) Å). Mn9 is in the 2+ oxidation state, has distorted octahedral geometry, and is bound to two μ_3 -oxides (Mn9–O20, 2.239(3) Å and Mn9–O20', 2.254(3) Å), two oxygens from DEA ligands (Mn9–O21', 2.110(4) Å and Mn9–O22, 2.109(4) Å) and two μ -chlorides (Mn9–Cl2, 2.497(14) Å and Mn9–Cl3, 2.492(14) Å) that bridge to Mn7 and Mn10 (Mn7–Cl2 distance given above, Mn10–Cl3, 2.531(15) Å). Finally, Mn10 is in the 2+ oxidation state, has distorted trigonal bipyramidal geometry, and is bound to the μ -chloride, a μ_3 -oxide (Mn10–O12', 2.029(3) Å), an oxygen atom of a DEA ligand (Mn10–O25, 2.152(4) Å), a phenolic oxygen (Mn10–O23, 2.122(4) Å) and a ligated dmf molecule (Mn10–O24, 2.126(4) Å).

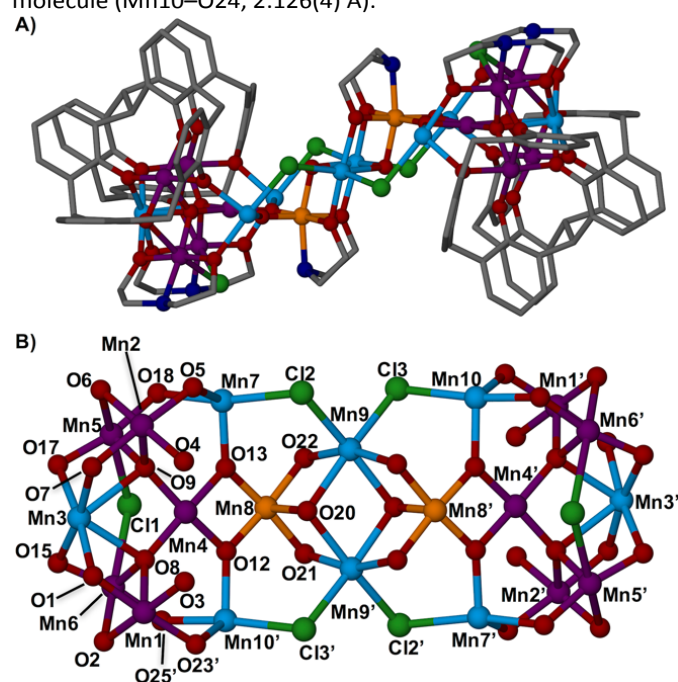


Fig. 3 A) Symmetry-expanded single crystal X-ray structure of **6**. B) top-down view of the cluster core in **6** showing the presence of a central Mn^{IV}₂Mn^{II}₂ butterfly. Selected atoms are labelled according to discussion. Colour code C – grey, O – red, N – royal blue, Mn^{II} – pale blue, Mn^{III} – purple, Mn^{IV} – orange, Cl – dark green. H atoms, ^tBu groups of L1, ligated solvent and co-crystallised solvent/anions are omitted.

Symmetry expansion of the ASU affords the entire cluster as shown in Figure 3A, which can be visualised as two Mn^{III}₅Mn^{II}₃ moieties linked *via* the central DEA-supported Mn^{IV}₂Mn^{II}₂ fragment. This fragment displays coordination modes that are typical for DEA and compound **6** can be considered an excellent example in which the nuclearity of clusters supported by one ligand type can be augmented (or greatly enhanced) *via* the incorporation of complementary and / or competing co-ligands; the complex topology of **6** (Fig. 3B) displays several recurring coordination modes typical for both L1-¹⁰ and DEA-supported clusters (Fig. S1).^{2b} Capping behaviour is observed with four [Mn^{III}(C[4])] moieties (Mn1,

Mn2 and s.e.) 'encapsulating' one Mn^{II} cation (Mn3) located in one of the binding pockets generated upon inversion of L1, whereas the other binding site remains unoccupied. This is unprecedented, and we propose that the strongly competing nature of DEA gives rise to this new structural feature; the presence of two additional DEA-supported Mn^{III} cations (Mn5 and Mn6) appears to create steric hindrance in that region of the cluster, preventing it from being occupied by a metal ion. This also reflects on the tetrahedral geometry of Mn4, which is unusual and unprecedented in L1-supported cluster chemistry thus far. A CSD search for Mn₂₀ clusters returned 18 hits with disparate topologies, the metallic cores of which are supported by a variety of ligands including phosphonate,¹⁸ triethanolamine,¹⁹ pivalate²⁰ and other N-containing polydentates.²¹ These clusters possess Mn ions in oxidation states between 1+ and 3+ in either mixed or non-mixed valence arrangements, but none were found to contain Mn^{IV} ions. The topology of **6** is thus found to be unique, as is the oxidation state distribution and mixed-valence arrangement. Inspection of the expanded structure of **6** shows that neighbouring clusters are well-isolated, with no significant intermolecular interactions being observed between symmetry equivalents; the shortest metal-metal inter-cluster distance is found between Mn1 and Mn7 ~12.1 Å along the crystallographic *b* axis (Fig. S2).

The dc (direct current) molar magnetic susceptibility, χ_M , of a freshly filtered polycrystalline sample of **6** was measured in an applied magnetic field, *B*, of 0.1 T, over the *T* = 5–300 K temperature range. The experimental results are shown in Figure S3 in the form of the $\chi_M T$ product versus *T*, where $\chi_M = M / B$, and *M* is the magnetisation of the sample. At room temperature, the $\chi_M T$ product is approximately 68 cm³ K mol⁻¹, in good agreement with the sum of Curie constants for a [Mn^{IV}₂Mn^{III}₁₀Mn^{II}₈] unit (68.75 cm³ K mol⁻¹, *g* = 2.0). Upon cooling, the $\chi_M T$ product decreases to a minimum value of 53.4 cm³ K mol⁻¹ at *T* = 34 K, then rises to a value of 58.3 cm³ K mol⁻¹ at *T* = 8 K, before decreasing again to a value of 57.5 cm³ K mol⁻¹ at *T* = 5 K. This behaviour is consistent with competing (weak) ferro- and antiferromagnetic exchange interactions between the Mn centres. The decrease in $\chi_M T$ below 8 K can be attributed to zero-field splitting effects and / or the presence of antiferromagnetic inter-molecular interactions. The large nuclearity and complex topology of the [Mn₂₀] core prevents any quantitative analysis of the exchange constants, but the overall behaviour is entirely consistent with that observed for other C[*n*]-constructed, O-atom bridged, heterovalent Mn cages, where typical coupling constants are of the order $|J| \leq 10$ cm⁻¹.^{22,23} Note also that $|J|$ is likely of the same order of magnitude as $|D_{Mn(III)}|$. The low temperature variable-temperature-and-variable-field (VTVB) magnetisation data collected in fields of up to *B* = 7 T (Fig. S3, inset) are also consistent with this picture, showing *M* increasing in a near linear fashion with *B*, without saturating (*M* = 44.7 μ_B at *T* = 2 K and *B* = 7 T). Complex **6** does not display any frequency-dependent signals in out-of-phase (χ_M'') ac susceptibility measurements, and is thus not an SMM.

In conclusion, we have shown that the use of BisTBC[4] with DEA as a co-ligand leads to the formation of a very high nuclearity mixed-valence Mn cluster that displays typical coordination modes relative to each ligand type. The competitive metal ion binding of DEA appears to influence that of BisTBC[4], and this delicate balance in ligand composition may be a route towards unearthing a large library of such cluster species in C[*n*] chemistry, whilst simultaneously increasing / enhancing metal ion composition. This will be achieved through the use of a library of DEA-based (as well as other tripodal) co-ligands, and is a strategy may also allow one to control the incorporation of metal ions with coordination numbers and oxidation states that are otherwise unobtainable using just BisTBC[4] as a ligand; this will likely apply to all C[*n*] ligands. This will have concomitant effects on the magnetic properties for these multi-component systems, the results of which will be reported in due course.

We thank Heriot-Watt University for financial support (MC, James Watt Studentship). EKB thanks the EPSRC. The Advanced Light Source is supported by the Director, Office of Science, Office of Basic Energy Sciences, of the US Department of Energy under contract no. DE-AC02-05CH11231. The authors report no conflicts of interest.

Notes and references

H₈L1 was synthesised according to literature procedure.¹²
Synthesis of [Mn^{IV}₂Mn^{III}₁₀Mn^{II}₈(L1)₂(DEA)₆(μ₄-O)₄(μ₃-O)₆(dmf)₁₀(Cl)₆(H₂O)₂](dmf)₂(MeOH)(H₂O)₃, **6: H₈L1** (500 mg, 0.39 mmol), MnCl₂·4H₂O (610 mg, 3.08 mmol) and diethanolamine (0.148 mL, 1.54 mmol) were suspended in a 1:1 dmf / MeOH mixture (20 mL) and stirred for 10 minutes. Et₃N (0.6 mL, XS) was added and the resulting purple solution was stirred for additional 2 hours and then filtered. The mother liquor was slowly allowed to diffuse with diethyl ether, affording dark purple crystals suitable for X-ray studies. Elemental Analysis (%) calculated for **6**, C₂₃₇H₃₅₀Mn₂₀N₁₈O₅₆Cl₆ (*M* = 5659): C, 50.3%; H, 6.23%; N, 4.46%. Found: C, 49.97%; H, 5.89%; N, 4.16%. **Yield** 404 mg (18 %). **Crystal Data for **6** (CCDC 1573336)**: C₂₃₇H₃₅₀Cl₆Mn₂₀N₁₈O₅₆, *M* = 5658.83 g/mol, monoclinic, space group C2/c (no. 15), *a* = 18.3953(7) Å, *b* = 45.6912(18) Å, *c* = 40.7908(16) Å, β = 99.212(2)°, *V* = 33843(2) Å³, *Z* = 4, *T* = 100(2) K, 163555 reflections measured (4.198° ≤ 2θ ≤ 58.238°), 34860 unique (*R*_{int} = 0.0610, *R*_σ = 0.0498) which were used in all calculations. The final *R*₁ was 0.0828 (*I* > 2σ(*I*)) and *wR*₂ was 0.2223 (all data).

- (a) G. Aromí and E. K. Brechin, *Struct. Bonding*, 2006, **122**, 1; (b) J.-N. Rebilly and T. Mallah, *Struct. Bonding*, 2006, **122**, 103; (c) G. Aromí, D. Aguila, P. Gamez, F. Luis and O. Roubeau, *Chem. Soc. Rev.*, 2012, **41**, 537; (d) E. J. L. McInnes, G. A. Timco, G. F. S. Whitehead and R. E. P. Winpenny, *Angew. Chem. Int. Ed.*, 2015, **54**, 14244; (e) C. J. Milios, T. C. Stamatatos and S. P. Perlepes, *Polyhedron*, 2006, **25**, 134; (f) L. N. Dawe, K. V. Shuvaev and L. K. Thompson, *Chem. Soc. Rev.*, 2009, **38**, 2334.
- (a) R. Saalfrank, T. Nakajima, N. Mooren, A. Scheurer, H. Maid, F. Hampel, C. Trieflinger, J. Daub, *Eur. J. Inorg. Chem.*, 2005, 1149; (b) A. J. Tasiopoulos and S. P. Perlepes, *Dalton Trans.*, 2008, 5537; (c) E. E. Moushi, A. Masello, W. Wernsdorfer, V. Nastopoulos, G. Christou and A. J. Tasiopoulos, *Dalton Trans.*, 2010, **39**, 4978; (d) S. K. Langley, C. Le, L. Ungur, B. Moubaraki, B. F. Abrahams, L. F. Chibotaru and K. S. Murray, *Inorg. Chem.*, 2015, **54**, 3631; (e) J. Rinck, Y.

- Lan, C. E. Anson and A. K. Powell, *Inorg. Chem.*, 2015, **54**, 3107.
- 3 (a) C. Aronica, G. Chastanet, E. Zueva, S. A. Borshch, J. M. Clemente-Juan, D. Luneau, *J. Am. Chem. Soc.*, 2008, **130**, 2365; (b) G. Karotsis, S. J. Teat, W. Wernsdorfer, S. Piligkos, S. J. Dalgarno, E. K. Brechin, *Angew. Chem. Int. Ed.*, 2009, **48**, 8285; (c) S. M. Taylor, G. Karotsis, R. D. McIntosh, S. Kennedy, S. J. Teat, C. M. Beavers, W. Wernsdorfer, S. Piligkos, S. J. Dalgarno, E. K. Brechin, *Chem. Eur. J.*, 2011, **17**, 7521; d) G. Karotsis, S. Kennedy, S. J. Dalgarno, E. K. Brechin, *Chem. Commun.* 2010, **46**, 3884; e) S. M. Aldoshin, I. S. Antipin, V. I. Ovcharenko, S. E. Solov'eva, A. S. Bogomyakov, D. V. Korchagin, G. V. Shilov, E. A. Yur'eva, F. B. Mushenok, K. V. Bozhenko, A. N. Utenyshev, *Russ. Chem. Bull.*, 2013, **62**, 536; f) S. M. Aldoshin, I. S. Antipin, S. E. Solov'eva, N. A. Sanina, D. V. Korchagin, G. V. Shilov, F. B. Mushenok, A. N. Utenyshev, K. V. Bozhenko, *J. Mol. Struct.*, 2015, **1081**, 217.
- 4 S. Sanz, R. D. McIntosh, C. M. Beavers, S. J. Teat, M. Evangelisti, E. K. Brechin, S. J. Dalgarno, *Chem. Commun.*, 2012, **48**, 1449.
- 5 (a) G. Karotsis, S. Kennedy, S. J. Teat, C. M. Beavers, D. A. Fowler, J. J. Morales, M. Evangelisti, S. J. Dalgarno, E. K. Brechin, *J. Am. Chem. Soc.*, 2010, **132**, 12983; (b) S. Sanz, K. Ferreira, R. D. McIntosh, S. J. Dalgarno, E. K. Brechin, *Chem. Commun.*, 2011, **47**, 9042.
- 6 M. Coletta, E. K. Brechin, S. J. Dalgarno, in *Calixarenes and Beyond*, ed. P. Neri, J. L. Sessler and M. -X. Wang, Springer International Publishing, Switzerland, 1st edn, 2016, ch. 25, pp 671–689.
- 7 E. K. Brechin, J. Yoo, M. Nakano, J. C. Huffman, D. N. Hendrickson, G. Christou, *Chem. Commun.*, 1999, 783.
- 8 Y. F. Bi, G. C. Xu, W. P. Liao, S. C. Du, R. P. Deng, B. W. Wang, *Sci. China. Chem.*, 2013, **55**, 967.
- 9 For example see: B. M. Furphy, J. M. Harrowfield, M. I. Ogden, B. W. Skelton, A. H. White, F. R. Wilner, *J. Chem. Soc., Dalton Trans.*, 1989, 2217; D. M. Homden, C. Redshaw, *Chem. Rev.*, 2008, **108**, 5086; C. Redshaw, *Dalton Trans.*, 2016, **45**, 9018.
- 10 For examples of recent reviews please see: T. Kajiwaru, N. Iki, M. Yamashita, *Coord. Chem. Rev.*, 2007, 251, 1734; Y. Bi, S. Du, W. Liao, *Coord. Chem. Rev.*, 2014, 276, 61.
- 11 K. Su, F. Jiang, J. Qian, J. Pan, J. Pang, X. Wan, F. Hu, M. Hong, *RSC Adv.*, 2015, **5**, 33579.
- 12 L. T. Carroll, P. Aru Hill, C. Q. Ngo, K. P. Klatt, J. L. Fantini, *Tetrahedron*, 2013, **69**, 5002.
- 13 P. Murphy, S. J. Dalgarno, M. J. Paterson, *J. Phys. Chem. A*, 2014, **118**, 7986.
- 14 R. McLellan, M. A. Palacios, C. M. Beavers, S. J. Teat, S. Piligkos, E. K. Brechin, S. J. Dalgarno, *Chem. Eur. J.*, 2015, **21**, 2804.
- 15 M. Coletta, R. McLellan, A. Waddington, S. Sanz, K. J. Gagnon, S. J. Teat, E. K. Brechin, S. J. Dalgarno, *Chem. Comm.*, 2016, **52**, 14246–14249.
- 16 M. Coletta, R. McLellan, S. Sanz, K. J. Gagnon, S. J. Teat, E. K. Brechin, S. J. Dalgarno, *Chem. Eur. J.*, 2017, **23**, 14073.
- 17 Crystals grew most readily from a 1:10:4 ratio of the reactants as described in the text, this being achieved through a combinatorial screen.
- 18 S. Maheswaran, G. Chastanet, S. J. Teat, T. Mallah, R. Sessoli, W. Wernsdorfer, R. E. P. Winpenny, *Angew. Chem. Int. Ed.*, 2005, **44**, 5044; M. Wang, C. Ma, H. Wen, C. Chen, *Dalton Trans.*, 2009, **0**, 994.
- 19 S. K. Langley, B. Moubaraki, K. J. Berry, K. S. Murray, *Dalton Trans.*, 2010, **39**, 4848.
- 20 N. Burkovskaya, G. Aleksandrov, E. Ugolkova, N. Efimov, I. Evstifeev, M. Kiskin, Z. Dobrokhotova, V. Minin, I. Eremenko, *New J. Chem.*, 2014, **38**, 1587.
- 21 R. Bagai, K. A. Abboud, G. Christou, *Inorg. Chem.*, 2008, **47**, 621.
- 22 M. A. Palacios, R. McLellan, C. M. Beavers, S. J. Teat, H. Weihe, S. Piligkos, S. J. Dalgarno, E. K. Brechin, *Chem. Eur. J.*, 2015, **21**, 11212.
- 23 R. McLellan, S. M. Taylor, R. D. McIntosh, E. K. Brechin, S. J. Dalgarno, *Dalton Trans.*, 2013, **42**, 6697.